Process description of SWQN

A simplified hydraulic model

A.A.M.F.R. Smit
C. Siderius
L.P.A van Gerwen

1

Alterra-Report 1226.1 ISSN 1566-7197

WAGENINGEN UR
For quality of life

Process description of SWQN

A simplified hydraulic model

A.A.M.F.R. Smit
C. Siderius
L.P.A. van Gerven

Alterra Report 1226.1

Alterra, Wageningen, 2009

ABSTRACT

Smit A.A.M.F.R., C. Siderius, L.P.A. van Gerven, 2009. Process description of SWQN; A simplified hydraulic model. Wageningen, Alterra Report 1226.1. 52 pp.; 12 figs.; 2 tables; 18 refs.

SWQN is a simplified hydraulic model for surface water systems which computes water levels and flows in a network of nodes labelled as 'volumes' and segments labelled as 'connectors'. The user can specify a variety of connectors like open water courses or structures such as weirs, gates, culverts or pumps. Water levels are calculated in the 'volumes' driving the one dimensional flows through the 'connectors' linking up the 'volumes'. The assumption is that the flow between two nodes with an open connection in between is linearly dependent on the difference in water level, if necessary augmented with the difference in velocity head, the wetted profile, and a given resistance. Each structure, on the other hand, has its own specific stage-discharge relation and is linearized using a number of intervals. The internal computational time step is usually set from one to several hours, but strongly depends on the water storage capacity associated with the volumes and the dynamic behaviour of the modelled system. SWQN has proven to be widely applicable and relatively fast for large networks.

Keywords: SWQN, surface water, hydraulics, model

ISSN 1566-7197

P.O. Box 47; 6700 AA Wageningen; The Netherlands
Phone: + 31 317 474700; fax: +31 317 419000; e-mail: info.alterra@wur.nl

Contents

Preface

The basic concepts of SWQN were formulated in 1984 at the start of the "Reuse of Drainage Water Project", a joint venture between the Drainage Research Institute, Cairo, Egypt, and the 'Instituut voor Cultuurtechniek en Waterhuishouding (ICW)', one of the predecessors of Alterra. WATDIS, as it was called in those days, formed an integral part of the SIWARE model package with which water management options in the Nile Delta were simulated for policy support of the Egyptian Ministry of Water Resources and Irrigation.

The reason to embark on developing such a model was the lack of knowledge and data on water distribution in the Nile Delta. Simplification of the hydraulic concepts was a prerequisite caused by the complexity and application scale of the SIWARE package together with limited hardware capacity at that stage of personal computing. Numerous calibrations that WATDIS could produce sufficiently accurate results.

In 2001 SWQN was wrapped in a new FORTRAN shell as part of the NL-CAT model package developed for the EU-EuroHarp project (www.euroharp.org). In EuroHarp a comparison was made between a number of European models simulating nutrients outflows at catchment scale. The NL-CAT package also formed the core of the Alterra instrument used in the Dutch government funded project "Monitoren Stroomgebieden" (www.monitoringstroomgebieden.nl). In this project water and nutrient flows were traced and analyzed in four typical Dutch water systems.

For further questions about the contents of this report the reader is referred to the authors Mr. A.A.M.F.R. Smit (robert.smit@wur.nl) and Mr. C. Siderius (christian.siderius@wur.nl).

Wageningen, September 2009

1 Introduction

Computing water levels and flows in very large schemes of open water courses requires a robust and relatively fast algorithm. To meet such requirements, Alterra has developed a model in which water courses are schematized into a network of nodes linked by segments. Water levels are computed in the nodes, whereas flows are calculated in the segments as a resultant of differences between water levels (and velocity head) in the adjacent nodes. The user can further specify structures, such as weirs, undershot gates, culverts, and pumps, in each of the segments.

The earliest versions were used to compute the water distribution in large irrigation schemes, such as the complete Nile Delta (Rijtema et al., 1991). Performance was so good in terms of computation time and accuracy (on that particular scale), that it was decided to derive a version which could also be used for Dutch catchments, where unlike the Nile Delta drainage is the dominant driver for surface water systems.
In order to fit in the new modeling framework developments at Alterra, it was decided to rebuild the original program into a Dynamic Link Library (DLL). Since then this DLL has been integrated in several software environments, such as the "Framework Integrated Water management" (Groenendijk et al., 1999), NL-CAT (Schoumans et al., 2009), and SWQN (Dik et al., 2009), where the abbreviation stands for Surface Water QuaNtity. SWQN is the most basic software application made up by the computational core and a shell handling in- and output.
SWQN has been successfully applied in a variety of areas, such as a number of Dutch polders and catchments (see: http://www.monitoringstroomgebieden.nl/ project phases 2 and 3, and Dik et al., 2004 and 2005) and several other catchments across Europe, like Odense in Denmark, Vansjo-Hobol in Norway and Zelivka in the Czech Republic (Schoumans et al., 2009). These catchments are all very different in topography, weather, and surface water management.

The simple and straightforward approach, robustness and computational efficiency makes SWQN a very useful tool for calculating water flows within a wide range of conditions. Nevertheless, the model also faces some limitations due to its simplifications of the basic St. Venant equations which describe the flow in open water conduits (Ven te Chow, 1959). It is not designed to deal with flows through pressure conduits, situations with rapidly varied flows, or large rivers in floodplains with a very irregular morphology where 2D-aspects are important. In this technical description and the user manual (Dik et al., 2009) the possibilities and restrictions of SWQN are further highlighted.

SWQN has been designed in a way that simplifies adding new functionality. The latest version allows for large network configurations up to thousands of nodes, depending on the internal memory of the computer used. The internal computational time step is usually set at one to several hours, but strongly depends on the water storage capacity associated with the volumes and the dynamic behavior of the modeled

system. Improvements in mathematical formulation and efficiency of algorithms are still ongoing.

This report describes in detail the computational core of SWQN. In Chapter 2 the theoretical background behind the simplification of the St. Venant equestions and the flow through weirs, culverts, gates and pumps is briefly explained. In Chapter 3 their implementation in SWQN is described, while Chapter 4 shows the solution scheme. Chapter 5 compares performance with other models by means of a mass-conservation and ramp-discharge test.
.

2 Theory

2.1 Flow in open conduits - St. Venant equations

The unsteady flow in open waters was first described by St. Venant in 1848. His well-known St. Venant equations consist of two parts: i) the conservation of mass and ii) the energy or momentum balance in one dimension for a water body of infinitesimal length. The St. Venant equations are the basis for the description of unsteady flow in open waters but require intricate numerical schemes to solve and are therefore not used in SWQN. In Annex 1 they are explained in more detailed. Here we explain the main assumptions and in the next paragraph describe the simplification which lead from the St. Venant equations to the equations used in SWQN.

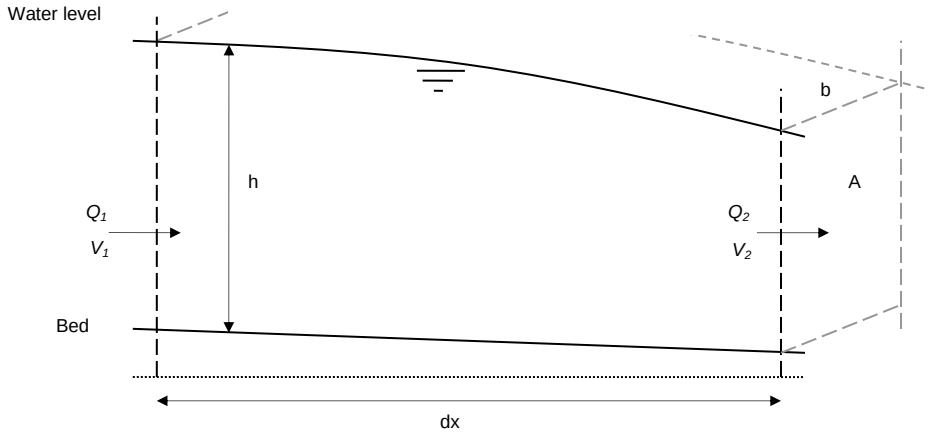

Figure 1 Flow through a part (dx) of the surface schematization

In Figure 1 a schematization of a short length (dx) of a prismatic surface water channel is shown. The continuity equation, describing the conservation of mass can be written as follows, when assuming no lateral inflow of water:

$$v\frac{\partial A}{\partial x} + A\frac{\partial v}{\partial x} + b\frac{\partial h}{\partial t} = 0 \qquad (1)$$

The dynamic (or momentum) equation, which constitutes the second part of the St. Venant equations and describes the energy or momentum balance in one dimension for a water body of infinitesimal length:

$$g\frac{\partial h}{\partial x} + v\frac{\partial v}{\partial x} + \frac{\partial v}{\partial t} = g(S_o - S_f) \qquad (2)$$

where:

A	cross sectional area	[m^2]
v	mean velocity at the section	[$m^2\ s^{-1}$]
b	width of the section	[m]
h	water level	[m]
t	time	[s]
g	acceleration due to gravity	[$m\ s^{-2}$]
S_o	bed slope	[-]
S_f	friction slope	[-]

Equations 1 and 2 together form the St. Venant equations describing unsteady flow in open waters. These dynamic wave equations are considered to be the most accurate and comprehensive solution to 1-D unsteady flow problems in open channels. Nonetheless, these equations are based on specific assumptions, and therefore have limitations. The assumptions used in deriving the dynamic wave equations are as follows:

- Velocity is constant and the water surface is horizontal *across* any channel section perpendicular to the longitudinal axis;
- All flows are gradually varied with hydrostatic pressure prevailing at all points along the longitudinal axis, such that vertical accelerations can be neglected;
- Channel boundaries are treated as fixed; therefore, no erosion or deposition occurs;
- The slope of the channel bottom is small;
- Water is of uniform density, and resistance to flow can be described by empirical formulas, such as the Manning or the Chézy equations;
- The flow is incompressible and homogeneous in density.

2.2 Simplification of the St. Venant equations

Due to their mathematical complexity exact integration of the St. Venant equations is practically impossible (Ven Te Chow, 1959). Instead they may be solved numerically, given one initial and two boundary conditions. Numerous flood routing methods exist which all use the continuity equation in a similar manner but differ in their use of the momentum equation (Weinmann and Laurenson, 1979). Models that retain all terms are called complete dynamic models. In SWQN, like in many other flood routing models, several terms are neglected. In the following paragraphs the steps taken to simplify the momentum equation are explained.

Equation 3 shows again the rewritten 2nd St. Venant or dynamic wave equation in a rearranged form. The first term describes the change in impulse over time, the second the net flux into the surface water section, and the third the change in pressure. S_o and S_f describe the friction and gravity forces working on the surface water section.

$$\frac{\partial v}{\partial t} + v\frac{\partial v}{\partial x} + g\frac{\partial h}{\partial x} - g(S_o - S_f) = 0 \qquad (3)$$

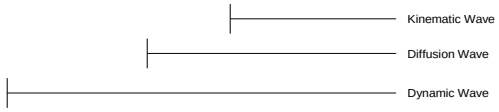

Not all terms in the dynamic equation are equal in size. Table 1 shows the relative importance of all terms related to the gravity force for a number of river catchments.

Table 1 Relative importance of all dynamic equations terms to the friction force for 5 catchments (derived from Torfs, 2000), where A comes from Henderson (1966) and B and C come from Weinmann and Laurenson, (1979)).

		Rhine	*Donau*	*A*	*B*	*C*
$g\,S_o$	Gravity	1	1	1	1	1
$g\,S_f$	Friction	≈1	≈1	≈1	≈1	≈1
$g\frac{\partial h}{\partial x}$	Pressure	-0.025	0.063	-0.019	-0.03	-0.85
$v\frac{\partial v}{\partial x}$	Impulse flux	0.001	0.004	0.0075	0.012	0.07
$\frac{\partial v}{\partial t}$	Change in impulse	-0.002	-0.002	-0.0019	-0.013	-0.06

From Table 1 it follows that several terms of the St. Venant equation may be disregarded without losing too much accuracy. When the impulse change and impulse flux are disregarded the dynamic equation changes in a diffusion wave description. When furthermore the pressure term is disregarded the equation describing a kinematic wave remains:

$$S_o = S_f \tag{4}$$

In the kinematic wave equation gravity and friction forces balance each other, or, in other words, the slope of the bed is equal to the friction slope. Using the well-known Chézy formula this friction slope can be described as:

$$S_f = \frac{v^2}{C^2 R} = \frac{Q^2}{C^2 A^2 R} \tag{3}$$

where

V	velocity	[m s^{-1}]
C	Chézy coefficient	[$m^{½}$ s^{-1}]
R	hydraulic radius	[m]
A	wetted cross profile of the segment	[m^2]

Combining Equation 4 with 5 gives:

$$Q = S_o^{½}\, C\, A R^{½} \tag{6}$$

Equation 6 describes the steady flow in open channels in which bed slope, water and energy levels are running parallel. To approximate non-uniform flows, the bottom slope in Equation 6 can be substituted by the slope of the water level in a longitudinal section j between points i and i+1:

$$S_{p,j,t} = \frac{\Delta h_{i,i+1,t}}{\Delta L_j} = \frac{\left(h_{i,t} - h_{i+1,t}\right)}{\Delta L_j} \tag{7}$$

with:

$S_{p,j,t}$	slope in pressure head for segment j at time t	[-]
$\Delta h_{i,i+1,t}$	difference in pressure head between nodes i and i+1	[m]
$h_{i,t}$	water level in node i	[m]
$h_{i+1,t}$	water level in node i+1	[m]
ΔL_j	distance between nodes i and i+1	[m]

This approach brings back the pressure term in the equations and, hence, approaches the diffusion wave (see Eq. 3). Using the slope of the water level is the default option in the SWQN module. The estimation can be further improved by substituting the bottom slope by the slope of the energy line (Eq. 8), so that the impulse flux is also covered by the equations and the dynamic wave is partially approximated. Optionally the model provides this possibility.

$$S_{e,j,t} = \frac{\Delta H_{i,i+1,t}}{\Delta L_j} = \frac{\left(h_{i,t} + \frac{v_{i,t}^2}{2g} - h_{i+1,t} - \frac{v_{i+1,t}^2}{2g} \right)}{\Delta L_j} \quad (8)$$

with

$S_{e,j,t}$	slope in energy head for segment j at time t	[-]
$\Delta H_{i,i+1,t}$	difference in energy head between nodes i and i+1	[m]
$h_{i,t}$	water level in node i	[m]
$h_{i+1,t}$	water level in node i+1	[m]
$v_{i,t}$	flow velocity in node i	[m s^{-1}]
$v_{i+1,t}$	flow velocity in node i+1	[m s^{-1}]
g	gravity constant	[m s^{-2}]
ΔL_j	distance between nodes i and i+1	[m]

There are some constraints to the above described simplifications in addition to the limitations of the second St. Venant equation as some terms in the dynamic wave are neglected or approximated. A fair example of such a constraint is a large flood wave in a gently sloping area or open waters where rapid variations in flow velocity over time occur at cross sections.Chapter 4 will go into detail on the consequences of the here described simplifications. Chapter 5 will give a comparison with other surface water models.

2.3 Structures

In many open water systems discharges are also influenced by structures like weirs and culverts. In the following paragraphs the basic relations for the most common structures are given as well as the approach to linearize the originally non-linear equations. The following four kinds of structures are presently described by SWQN:

- Weir
- Undershot gate
- Culvert
- Pump

Other types such as siphons can be easily added to the model code, if needed.

2.3.1 Weir

Weirs are predominantly used for upstream water level control, but can also be used for water distribution and flow measurements. A large variety of differently shaped and weirs with fixed and movable crests exist. In SWQN only rectangular weirs are accounted for. The general stage-discharge relation for a rectangular broad crested weirs reads (CTV, 1988, and Figure 2 left):

$$Q_{weir,t} = C_d\ C_v\ (\tfrac{2}{3})^{1.5}\ (g)^{0.5}\ W_{crest}\ (h_{up,t} - h_{crest,t})^{1.5} \quad (4)$$

where:

$Q_{weir,t}$	weir discharge at time t	[$m^3\ s^{-1}$]
C_d	discharge efficiency coefficient	[-]
C_v	velocity correction coefficient	[-]
W_{crest}	crest width	[m]
$h_{up,t}$	upstream water level	[m]
$h_{crest,t}$	crest level	[m]
g	gravity constant	[$m \cdot s^{-2}$]

A similar equations applies for sharp crested weirs (CTV, 1988, and Figure 2 middle):

$$Q_{weir,t} = C_{d'}\ C_{v'}\ \delta\ \tfrac{2}{3}\ (2g)^{0.5}\ W_{crest}\ (h_{up,t} - h_{crest,t})^{1.5} \quad (5)$$

where:

δ	contraction coefficient	[-]

The discharge efficiency coefficient C_d is usually estimated between 1.0 and 1.25 for a sharp crested weir and 0.848 for a broad crested weir under common flow conditions (CTV, 1988). This coefficient, however, will be influenced significantly by the crest shape of the sharp crested weir and the degree of aeration. The velocity correction coefficient C_v ranges from 1.0 to 1.1 for sharp and broad crested weirs, respectively (Bos, 1978). The contraction coefficient is often set at unity.

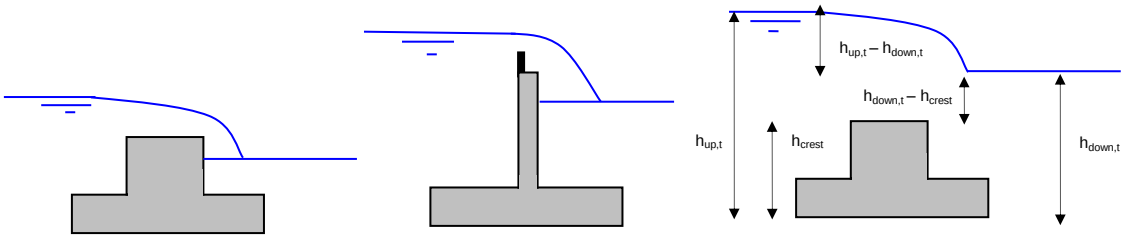

Figure 2 Broad crested weir (left), sharp crested weir (middle), and submerged weir (right)

A special case exists when the water level at the downstream side rises above the crest level (Figure 2 right). In such cases the weir is considered drowned and Equation 9 is combined with an equation for submerged flow through an orifice as presented in Equation 22:

$$Q_{weir,t} = C_{d''}\ C_{v''}\ W_{crest} \left[(\tfrac{2}{3})(2g)^{0.5}\ (h_{up,t} - h_{down,t})^{1.5} + (2g)^{0.5}\ (h_{down,t} - h_{crest,t})(h_{up,t} - h_{down,t})^{0.5} \right] \quad (6)$$

The first part of Equation 11 represents the free flow over a weir where h_{crest} is replaced by $h_{down,t}$ (see also Figure 2). The second part describes the submerged flow over the weir, where the submerged part is given by $(h_{up,t} - h_{down,t})$.

2.3.2 Undershot gate

Undershot gates are classified as an opening in a plate or a bulkhead of which the top is placed well below the upstream water level. They are used for water regulation. Depending on up- and downstream water levels, five different situations of stage-discharge relations can be distinguished as illustrated in Figure 3:

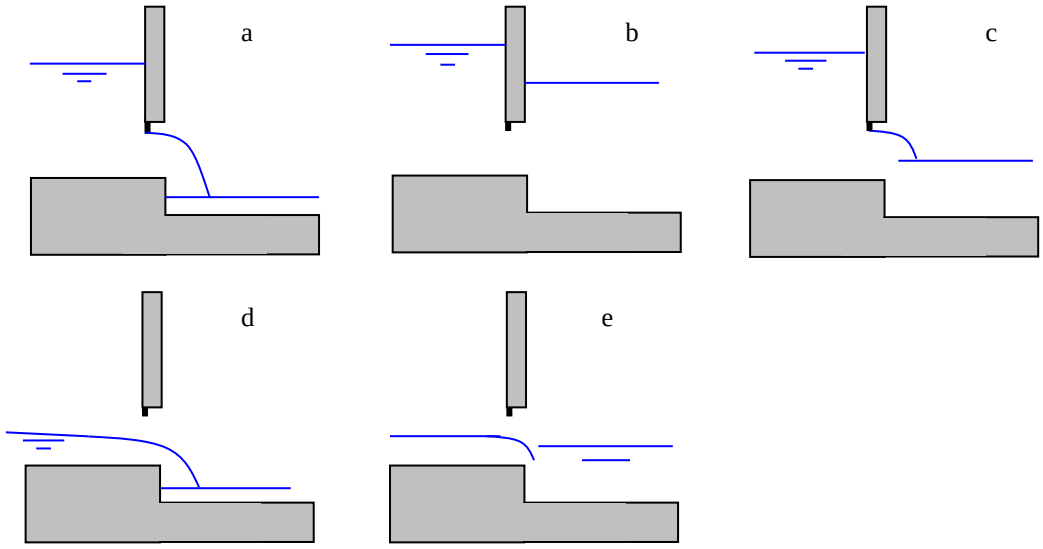

Figure 3 Freely discharging underflow (a), submerged underflow (b), partially submerged underflow (c), freely discharging broad crested weir type of flow (d), and submerged broad crested weir type of flow (e).

Each of these situations can be expressed as follows:

a) Freely discharging orifice (Gelok, 1969):

$$Q_{undershot,t} = C_d \, C_v \, (2g)^{0.5} \, A_{undershot,t} \, (h_{up,t} - h_{centre,t})^{0.5} \qquad (7)$$

with:

$Q_{undershot,t}$	discharge of free flow undershot gate at time t	[$m^3 \cdot s^{-1}$]
C_d	discharge efficiency coefficient usually estimated at 0.61	[-]
C_v	velocity correction coefficient usually estimated at 1.035	[-]
$A_{undershot,t}$	variable gate opening at time t	[m^2]
$h_{centre,t}$	level of the centre of the gate opening at the upstream side at time t	[m]

b) Fully submerged orifices (CTV, 1988):

$$Q_{undershott} = C_{d'}\, C_{v'}\, (2g)^{0.5}\, A_{undershott}\, \left(h_{up,t} - h_{down,t}\right)^{0.5} \quad (8)$$

c) Partially submerged orifices with a downstream water level below the top of the gate opening (CTV, 1988):

$$Q_{undershott} = C_{d''}\, C_{v''}\, (2g)^{0.5}\, A_{undershott}\, \left(h_{up,t} - h_{centre,t}\right)^{0.5} \quad (9)$$

d-e) In case both upstream and downstream water levels drop below the top of the gate opening, the structure no longer performs as an orifice but functions as a broad crested weir and Equation 9 then applies.

2.3.3 Culvert

Culverts are closed conduits generally used to under cross other infrastructure, such as roads, waterways, railroads, etc. Generally, no water level or flow control mechanisms are present. Various shapes exist and culverts are built with different construction materials. For straight culverts a similar equation as for undershot gates under submerged conditions is used (Equation 13) in which the coefficients C_d and C_v are replaced by a single resistance coefficient μ (Gelok, 1969; CTV, 1988):

$$Q_{culvert,t} = \mu \cdot (2g)^{0.5} A_{culvert} \left(h_{up,t} - h_{down,t}\right)^{0.5} \quad (10)$$

with:

$$\mu = \frac{1}{\sqrt{\xi_e + \xi_f + \xi_o}} \quad (11)$$

where:

μ	combined resistance coefficient	[-]
$A_{culvert}$	cross sectional area of the culvert	[m^2]
ξ_e	entry resistance coefficient	[-]
ξ_f	friction coefficient	[-]
ξ_o	coefficient for outlet losses	[-]

The CTV (1988) gives as entry resistance coefficient values of approximately 0.6 for round shaped culverts and 0.5 for square shaped culverts. The friction coefficient is calculated according to Equation 26 as a function of the length, hydraulic radius, and Manning roughness coefficient, usually set at 75 (Ven Te Chow, 1959; CTV, 1988). No provisions are made for curved culverts in Equation 16, but a ξ_b could easily be

added to the square rooted denominator, while values could be retrieved from tables (CTV, 1988).

$$\xi_f = \frac{2g\,L}{k_M{}^2\,R^{4/3}} \tag{12}$$

where:

L	length of culvert	[m]
k_M	Manning coefficient	[$m^{1/3}\ s^{-1}$]
R	hydraulic radius	[m]

The coefficient for energy losses at the outlet depends on the ratio between wetted cross section of the culvert and cross section of the downstream water course as described in the CTV (1988):

$$\xi_o = \left(1 - a\alpha\right)^2 k \tag{13}$$

where:

a	number of parallel culverts	[-]
α	wetted cross profile of the culvert divided by the wetted cross profile of the downstream water course	[-]
k	shape coefficient for the outlet	[-]

The value for k is set at unity if all kinetic energy is dissipated at the outlet. If no energy losses occur k can be set at zero.

2.3.4 Pump

Pumps are usually found at locations where a negative head has to be bridged in the water system. This is often the case in (low-lying) polders where excess water has to be pumped out to higher elevated water courses. In such areas, operators or automated systems generally exercise control by observing water levels at the upstream side, i.e. a start level at which the pump starts and a stop level at which pumping is ceased. Another example for the use of pumps can be found in irrigated agriculture where a certain downstream demand has to be met and flow control instead of level control is usually practiced.

Different types of pumps can be found each with their own advantages and disadvantages. Discharge may depend on the water levels at the suction and/or supply side, but for most pumps the relation between head and discharge does not deviate too much from linearity. Hence, SWQN either uses a linear relation or a constant discharge.

3. Implementation

3.1 Introduction

The SWQN module provides a method to compute flows and water levels in a schematized network of nodes labeled as 'volumes' and segments labeled as 'connectors'. Water levels are calculated in the nodes and the differences in water levels between connected nodes form the driving force behind the one-dimensional flow.

The module is pseudo-dynamic in time, assuming that steady-state conditions prevail during a time step. A connector can be specified as an open watercourse or a structure like a weir, gate, pump, etc. It is assumed that the flow between two nodes is linearly dependent on the difference in water level (if desired with the velocity head included), the wetted profile, and a given resistance. Each structure has its own specific stage-discharge relation and is linearized using a number of intervals.

The model is designed in a way that simplifies the addition of new functionality. Both the data transfer (through a structure block), and the internal structure of the model are prepared for this. New functionality will chiefly consist of different types of structures. The latest version allows for large network configurations up to several thousands of nodes, depending on the internal memory of the computer used and an acceptable computation time. The internal time step is usually set from one to several hours, but strongly depends on the water storage capacity associated with the volumes and the dynamic behavior of the modeled system.

3.2 Nodes

Each node in the network of water courses is associated with a storage volume. The nodes are the basic computational elements with a water level variable in time depending on the storage capacity and driven by in- and outgoing flows and boundary conditions, such as drainage, precipitation and evaporation. The actual water volume of a node is calculated based on the water depth in the node times half the surface water area of each connected segment (Figure 4).

Hence, the basic equation for a node i follows mass conservation and reads:

$$\frac{dV_i}{dt} = \frac{d\left(A_{surface,i}\, h_i\right)}{dt} = Q_{i-1,i} - Q_{i,i+1} - \Sigma Q_i \qquad (14)$$

where:

V_i	water volume in node i at time t	[m^3]
$A_{surface,i}$	water surface area of node i	[m^2]
h_i	water level in node i	[m]

dt	time step	[s]
$Q_{i-1,i}$	flow from node i-1 to node i	[$m^3 \cdot s^{-1}$]
$Q_{i,i+1}$	flow from node i to node i+1	[$m^3 \cdot s^{-1}$]
ΣQ_i	sum of sink and/or source terms for node i	[$m^3 \cdot s^{-1}$]

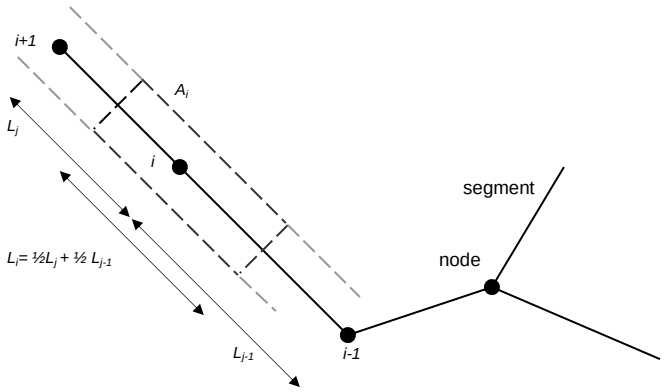

Figure 4 schematization in nodes and sections

The surface water area of a node is calculated by multiplying half the section length times the width of the water area for each segment connected to the node after which they are all added up.

In trapezoid channel segments the water surface is a function of the water level which can be expressed for k connected segments as:

$$A_{surface,i} = \sum_{j=1}^{k} \frac{1}{2} \Delta L_j \, B_j \, 2n_j \, h_i \qquad (15)$$

with:

ΔL_j	length of segment j	[m]
B_j	bottom width of the segment j cross profile	[m]
n_j	side slope of the segment j cross profile	[-]

For other cross shapes other functions will apply for $A_{surface}$.
Sink and source terms may occur simultaneously and may be constant or time dependent. These terms are usually considered as boundary conditions (Paragraph 3.4) and may represent for instance:

- Precipitation
- Open water evaporation
- Drainage from and infiltration into the subsoil
- Run-off from the topsoil and/or subsurface drainage
- Leakage to and seepage from the groundwater

3.3 Segments

Nodes are connected by segments and each node can be linked up to ten other nodes. As shown in the previous chapter, the segments currently implemented in the SWQN module are:

- Open connection
- Weir
- Undershot gate
- Culvert
- Pump

3.3.1 Open connection

The most commonly used connector is the open connection. The flow profile of an open connection may have various shapes as referred to in Paragraph 3.2. In the present version of the model, however, it is composed of linear line pieces. A widely used profile is the trapezoid. When describing the flow of water from one node to another through a segment *j*, while assuming uniform and steady-state flow conditions during a time step, Equation 6 can be written as:

$$Q_{j,t} = C_{Chezy,j}\, A_{j,t} \sqrt{R_{j,t}\, s_j} \qquad (16)$$

where:

$Q_{j,t}$	flow in segment j at time t	[$m^3 s^{-1}$]
$C_{Chézy,j}$	de Chézy coefficient for segment j	[$m^{1/2} s^{-1}$]
$A_{j,t}$	wetted cross profile of segment j	[m^2]
$R_{j,t}$	hydraulic radius of segment j	[m]
s_j	slope in bottom level (longitudinal)	[-]

As flows are generally non-uniform, the bottom slope s_j can be substituted by either Equations 7 or 16, where the former is used as default in SWQN as common flow velocities are rather low.

Chézy or Manning
A choice can be made between different friction coefficients, i.e. either the previously mentioned Chézy coefficient or the Manning coefficient k_m. In the latter case SWQN converts k_m into a Chézy coefficient using:

$$C_{Chezy} = R^{1/6} k_m \qquad (17)$$

where:

k_m	Manning coefficient	[$m^{1/3} s^{-1}$]

Linearization
It is assumed that over relatively small time steps and small distances the flow Q can be approximated by taking the difference in water level as the 'driving force'. Such an assumption would also yield a simple and quick numerical solution scheme. The principally non-linear flow Equation 6, combined with Equation 7, is therefore rewritten into a constant coefficient and a linear function in h following:

$$Q_{j,t} = C^*_{j,t}\ \Delta h_{j,t} \tag{18}$$

with:

$$C^*_{j,t} = C_{Chezy,j}\ A_{j,t} \sqrt{\frac{R_{j,t}}{\Delta h_{j,t-1}\ \Delta L_j}} \tag{19}$$

$$\Delta h_{j,t} = h_{i,t} - h_{i+1,t} \tag{20}$$

in which:

$\Delta h_{j,t-1}$	difference in water level over segment j at the previous time step	[m]

The wetted cross section and hydraulic radius of the segment are based on average values for slope and bottom width given at the beginning and end of each segment. As can be seen from Equation 24 Δh is still present in coefficient $C^*_{j,t}$. Nevertheless flow equation 23 can be considered as linear to $\Delta h_{j,t}$ because Δh is taken from the previous time-step ($\Delta h_{j,t-1}$) and is thus considered constant for the present time step.

3.3.2 Weir

In the surface water module Equation 9 describing free flow over a weir is simplified to:

$$Q_{weir,t} = \mu_{weir}\ W_{crest}\ \left(h_{i,t} - h_{crest,t}\right)^{1.5} \tag{21}$$

with

$$\mu_{weir,broadcrested} = C_d\ C_v\ \tfrac{2}{3}\left(\tfrac{2}{3}\ g\right)^{0.5} \tag{22}$$

$$\mu_{weir,sharpcrested} = C_{d'}\ C_{v'}\ \tfrac{2}{3}\left(2g\right)^{0.5} \tag{23}$$

in which:

$h_{i,t}$	Upstream water level (h_{up})	[m]
μ_{weir}	Weir type dependent resistance	[$m^{0.5}\ s^{-1}$]

μ_{weir} is the user defined resistance, a combination of the discharge efficiency and velocity correction coefficients (C_d and C_v), which can be specified for sharp or broad

crested weirs using the various known discharge coefficients as described in Paragraph 2.2.1.

A special case exists when the water level at the downstream side rises above the crest level and the weir becomes drowned. Under such conditions Equation 29 applies, which is assembled from Equations 35 and 36 (or 37) for the 'free flowing' part and Equation 46 for the 'submerged flowing' part:

$$Q_{weir,t} = W_{crest} \left[\mu_{weir} \left(h_{i,t} - h_{i+1,t} \right)^{1.5} + \mu_{gate} \left(h_{i+1,t} - h_{crest} \right) \left(h_{i,t} - h_{i+1,t} \right)^{0.5} \right] \quad (24)$$

Linearization for a free flowing weir
From Equation 26 it follows that for a maximum weir discharge:

$$Q_{weir,\max} = \mu_{weir} W_{crest} \left(h_{i,\max} - h_{crest,\min} \right)^{1.5} \quad (25)$$

with:

$Q_{weir,max}$	Maximum weir discharge	[$m^3 s^{-1}$]
$h_{i,max}$	Maximum upstream water level	[m]
$h_{crest,min}$	Minimum crest level	[m]

Combining both Equations 26 and 30 yields:

$$\frac{Q_{weir,t}}{Q_{weir,\max}} = \left(\frac{h_{i,t} - h_{crest,t}}{h_{i,\max} - h_{crest,\min}} \right)^{1.5} \quad (26)$$

This power function can now be piece-wise linearized into a number of intervals using:

$$Q_{weir,t,linear} = a_n Q_{weir,\max} + b_n Q_{weir,\max} \left(\frac{h_{i,t} - h_{crest,t}}{h_{i,\max} - h_{crest,\min}} \right) \quad (27)$$

where:

$Q_{weir,t,linear}$	Linearized weir discharge	[$m^3 s^{-1}$]
a_n	Linearization factor	[-]
b_n	Linearization factor	[-]

Figure 5 presents an example of the general shape of the equation and the use of intervals. The linearization is divided in three parts between 'no flow', when the water level is at or below the lowest crest level, and 'maximum flow', when crest level is at its minimum and water level is at its maximum level.

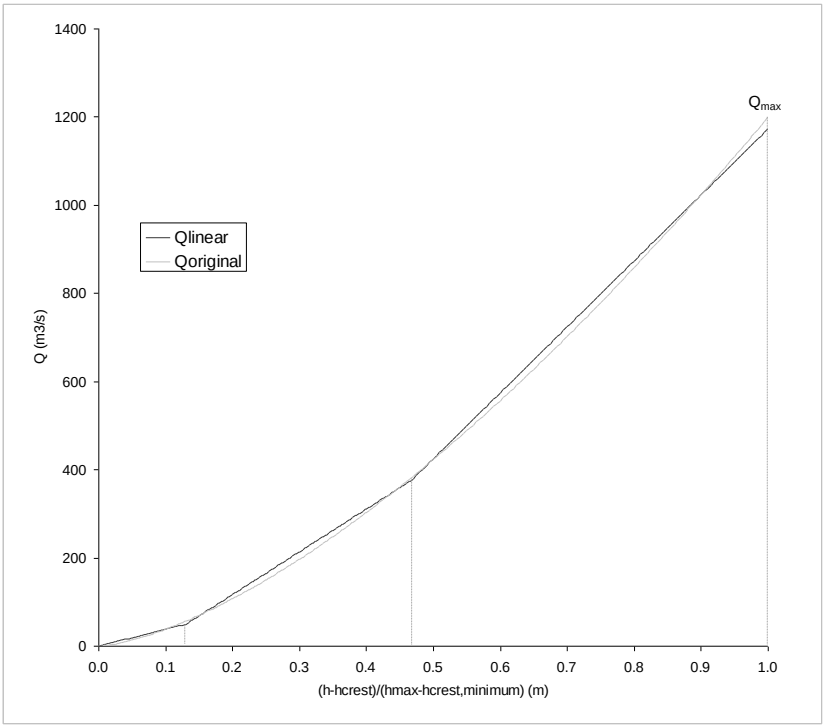

Figure 5 Example of a three-stage linearization for the stage-discharge relation of a weir

The three stages for the linearization of the stage-discharge relation for freely discharging weirs are:

- stage 1: $0.000 \le \frac{h_{i,t} - h_{crest,t}}{h_{i,\max} - h_{crest,\min}} \le 0.131$, with a=0 and b=0.3175
- stage 2: $0.131 \le \frac{h_{i,t} - h_{crest,t}}{h_{i,\max} - h_{crest,\min}} \le 0.467$, with a=-0.0641 and b=0.8084
- stage 3: $0.467 \le \frac{h_{i,t} - h_{crest,t}}{h_{i,\max} - h_{crest,\min}} \le 1.000$, with a=-0.269 and b=1.2471

It is important that the trajectory $h_{i,max} - h_{crest,min}$ covers the range of calculated water levels. In case no maximum water levels are known, the soil surface can be taken as an approximation. When the water level exceeds $h_{i,max}$ the discharge is calculated by extrapolation of stage 3.

Linearization for a submerged weir
For the submerged weir the maximum discharge can be expressed in analogy to Equation 30, which combined with Equation 29 results in:

$$\frac{Q_{weir,t}}{Q_{weir,\max}} = \left(\frac{h_{i,t} - h_{crest,t}}{h_{i,\max} - h_{crest,\min}} \right)^{1.5} \cdot \left[\left(1 - \frac{h_{i+1,t} - h_{crest,t}}{h_{i,t} - h_{crest,t}} \right)^{1.5} + \delta \left(\left(\frac{h_{i+1,t} - h_{crest,t}}{h_{i,t} - h_{crest,t}} \right)^{2} - \left(\frac{h_{i+1,t} - h_{crest,t}}{h_{i,t} - h_{crest,t}} \right)^{3} \right)^{0.5} \right] \quad (28)$$

with:

$$\delta = \frac{\mu_{gate}}{\mu_{weir}}$$

The first part of this equation expresses the flow over a freely discharging weir, while the latter part gives a correction function for submerged conditions:

$$\frac{Q_{weir,t}}{Q_{weir,\max}} = \left(\frac{h_{i,t} - h_{crest,t}}{h_{i,\max} - h_{crest,\min}} \right)^{1.5} \cdot \delta \left(\left(\frac{h_{i+1,t} - h_{crest,t}}{h_{i,t} - h_{crest,t}} \right)^{2} - \left(\frac{h_{i+1,t} - h_{crest,t}}{h_{i,t} - h_{crest,t}} \right)^{3} \right)^{0.5} \quad (29)$$

Equation 42 is then linearized in four stages using Equation 41 for the first part and the following linear function $c_{f,t}$ is used for the second part (Equation 43):

$$c_{f,t} = c + d \left(\frac{h_{i+1,t} - h_{crest,t}}{h_{i,t} - h_{crest,t}} \right) \quad (30)$$

where following conditions for the constants c and d apply:

- stage 1: $0.0 \le \frac{h_{i+1,t} - h_{crest,t}}{h_{i,t} - h_{crest,t}} \le 0.3$, with c=1.0 and d=0.0
- stage 2: $0.3 \le \frac{h_{i+1,t} - h_{crest,t}}{h_{i,t} - h_{crest,t}} \le 0.6$, with c=1.45 and d=-0.483
- stage 3: $0.6 \le \frac{h_{i+1,t} - h_{crest,t}}{h_{i,t} - h_{crest,t}} \le 0.9$, with c=1.505 and d=-1.083
- stage 4: $0.9 \le \frac{h_{i+1,t} - h_{crest,t}}{h_{i,t} - h_{crest,t}} \le 1.0$, with c=5.300 and d=-5.300

The correlation between the original and linearized flow functions is well above 0.999. Multiplication of the linearized free flow function and linearized correction function gives the linearized submerged flow function.

Level control
Level control is usually exercised by adjusting the crest on top of the weir between a minimum and a maximum level. The model allows for the following controls:

- Upstream water level $h_{i,t,target}$ set for a given period in time;
- Downstream water level $h_{i+1,t,target}$ set for a given period in time;
- Crest level $h_{crest,t,}$ set for a given period in time.

For the first two control settings a new crest level is determined based on the old level plus the difference in level between the given target level and the actual water level. For upstream control:

$$h_{weir,t} = h_{weir,t_0} + f_{damp}\left(h_{weir,target} - h_i\right) \quad (31)$$

and for downstream control:

$$h_{weir,t} = h_{weir,t_0} - f_{damp}\left(h_{weir,target} - h_{i+1}\right) \quad (37)$$

with:

$h_{weir,t}$	New weir level	[m]
h_{weir,t_o}	Weir level of previous time step	[m]
h_{target}	Target weir level	[m]
f_{damp}	Damping factor	[-]

The damping factor f_{damp} makes sure that weir levels do not fluctuate too rapidly and is based on empirical model use. Especially for wide broad weirs a small fluctuation in water can cause a large in- or decrease in discharge. The f_{damp} is therefore set as a function of the crest width:

$$f_{damp} = \frac{1}{\left(2 + W_{crest}\right)} \quad (32)$$

A fixed crest level can always be assigned directly to the model.

3.3.3 Undershot gate/orifice

The stage-discharge relations for gates can also be further simplified following the different states of up- and downstream water levels:

a) The flow through a freely discharging orifice can be written as (see Fig. 4a):

$$Q_{gate,t} = \mu_{free}\ A_{gate,t}\ \left(h_{i,t} - h_{centre,t}\right)^{0.5} \quad (33)$$

with:

$$\mu_{free} = C_d \; C_v \; (2g)^{0.5} \tag{40}$$

b) For fully submerged orifices the stage-discharge equation reads (Fig. 4b):

$$Q_{gate,t} \quad = \quad \mu_{sub} \; A_{gate,t} \; \left(h_{i,t} - h_{i+1,t}\right)^{0.5} \tag{34}$$

with

$$\mu_{sub} = C_{d'} \; C_{v'} \; (2g)^{0.5} \tag{35}$$

c) While for partially submerged orifices the stage-discharge equation reads (Fig. 4c):

$$Q_{gate,t} \quad = \quad \mu_{part.sub} \; A_{gate,t} \; \left(h_{i,t} - h_{centre,t}\right)^{0.5} \tag{36}$$

with

$$\mu_{part.sub} = C_{d''} \; C_{v''} \; (2g)^{0.5} \tag{37}$$

d) In case the upstream water level drops below the top of the gate opening, the structure no longer performs as an orifice but functions as a weir and Equation 26 then applies with accompanying linearizations.

Linearization
The linearization methodology followed for undershot gates is comparable to the one presented for weirs. Distinction has to be made between freely discharging and submerged gates, where partially submerged structures can be combined with freely discharging orifices.
From Equation 39 maximum discharge pertaining to freely and partially submerged orifices can be calculated as:

$$Q_{gate,\max} \quad = \quad \mu \; A_{gate,\max} \; \left(h_{i,\max} - h_{centre,gate-\max}\right)^{0.5} \tag{38}$$

with:

$Q_{gate,max}$	Maximum discharge through orifice	[$m^3 \cdot s^{-1}$]
$A_{gate,max}$	Maximum opening of the orifice	[m]
$h_{centre,gate-max}$	Centre of orifice at maximum gate opening	[m]

Combining Equations 39 and 45 results in:

$$\frac{Q_{gate,t}}{Q_{gate,\max}} = \frac{A_{gate,t}}{A_{gate,\max}} \left(\frac{h_{i,t} - h_{centre,t}}{h_{i,\max} - h_{centre,gate-\max}} \right)^{0.5} \tag{39}$$

which subsequently can be linearized as:

$$Q_{gate,t,linear} = a\, Q_{gate,max} \frac{A_{gate,t}}{A_{gate,max}} + b\, Q_{gate,\max} \frac{A_{gate,t}}{A_{gate,max}} \left(\frac{h_{i,t} - h_{centre,t}}{h_{i,max} - h_{centre,gate-\max}} \right) \tag{40}$$

where:

$Q_{gate,linear}$	Linearized gate discharge	[$m^3 \cdot s^{-1}$]
a	Linearization factor	[-]
b	Linearization factor	[-]

The four stages for piece-wise linearization of the stage-discharge relation for freely discharging or partially submerged gates are:

- stage 1: $0.000 \le \frac{h_{i,t} - h_{centre,t}}{h_{i,\max} - h_{centre,gate-\max}} \le 0.028$, with a=0 and b=7.050
- stage 2: $0.028 \le \frac{h_{i,t} - h_{centre,t}}{h_{i,\max} - h_{centre,gate-\max}} \le 0.158$, with a=0.159 and b=1.461
- stage 3: $0.158 \le \frac{h_{i,t} - h_{centre,t}}{h_{i,\max} - h_{centre,gate-\max}} \le 0.404$, with a=0.224 and b=1.049
- stage 4: $0.404 \le \frac{h_{i,t} - h_{centre,t}}{h_{i,\max} - h_{centre,gate-\max}} \le 1.000$, with a=0.401 and b=0.610

A similar approach is taken for the submerged gates:

$$Q_{gate,\max} = \mu_{sub}\, A_{gate,\max} \left(h_{i,\max} - h_{i+1,\min} \right)^{0.5} \tag{41}$$

where:

$h_{i+1,min}$	Minimum downstream water level (but above orifice)	[m]

which results in:

$$\frac{Q_{gate,t}}{Q_{gate,\max}} = \frac{A_{gate,t}}{A_{gate,\max}} \left(\frac{h_{i,t} - h_{i+1,t}}{h_{i,\max} - h_{i+1,\min}} \right)^{0.5} \tag{42}$$

and which subsequently can be linearized as:

$$Q_{gate,t,linear} = a\, Q_{gate,max} \frac{A_{gate,t}}{A_{gate,max}} + b\, Q_{gate,\max} \frac{A_{gate,t}}{A_{gate,max}} \left(\frac{h_{i,t} - h_{i+1,t}}{h_{i,max} - h_{i+1,\min}} \right) \qquad (43)$$

The four stages for piece-wise linearization of the stage-discharge relation for a submerged gate are finally:

- stage 1: $0.000 \le \frac{h_{i,t} - h_{i+1,t}}{h_{i,\max} - h_{i+1,\min}} \le 0.028$, with a=0 and b= 7.050
- stage 2: $0.028 \le \frac{h_{i,t} - h_{i+1,t}}{h_{i,\max} - h_{i+1,\min}} \le 0.158$, with a=0.159 and b= 1.461
- stage 3: $0.158 \le \frac{h_{i,t} - h_{i+1,t}}{h_{i,\max} - h_{i+1,\min}} \le 0.404$, with a=0.224 and b=1.049
- stage 4: $0.404 \le \frac{h_{i,t} - h_{i+1,t}}{h_{i,\max} - h_{i+1,\min}} \le 1.000$, with a=0.401 and b=0.610

The correlation between both power functions and their linear approximations is higher than 0.999.

Level control

Level control is implemented by adjusting the vertical gate opening between a given minimum and maximum level. In the model four types of control can be set for a defined period in time:

- Upstream water level $h_{i,t,target}$
- Downstream water level $h_{i+1,t,target}$
- Upstream water level and downstream water level simultaneously
- Bottom level of the movable gate

For up- or downstream water level control a new gate opening is determined based on Equation 51. The formula used for simultaneous up- and downstream control is given in Equation 52. A fixed bottom level of the movable gate can be supplied directly to the model.

$$h_{bottomgate,t} = \sqrt{1 - \frac{h_{i,t,target} - h_{i,t}}{Max\left(h_{i,t,target}, h_{i,t}\right)}}\; h_{bottomgate,t_0} \qquad (44)$$

$$h_{bottomgate,t} = \sqrt{1 - \frac{h_{i,t,target} - h_{i,t}}{Max\left(h_{i,t,target}, h_{i,t}\right)} + \frac{h_{i+1,t,target} - h_{i+1,t}}{Max\left(h_{i+1,t,target}, h_{i+1,t}\right)}}\; h_{bottomgate,t_0} \qquad (45)$$

3.3.4 Culvert

Two kinds of culverts can be defined, square and round ones. Depending on the type of culvert, the width or diameter has to be defined. For the implementation of the culverts in SWQN the resistance coefficients are reduced to the most important term, the friction coefficient. The inflow and outflow resistance terms are thus neglected. The stage-discharge equation then reads:

$$Q_{culvert,t} = \mu'_{culvert} A_{culvert,t} \left(h_{i,t} - h_{culvert,t}\right)^{0.5} \quad (46)$$

with:

$$\mu'_{culvert} = \frac{k_M{}^2 R^{4/3}}{L} \quad (47)$$

where:

$\mu'_{culvert}$ Lumped resistance factor for culverts [-]

The Manning friction coefficient has to be defined by the user. Values for the Manning friction coefficient for concrete culverts are given by Ven Te Chow (1959) and the CTV (1988).

Linearization is similar to the approach followed for a freely discharging gate.

3.3.5 Pump

The stage-discharge relation for pumps is simplified to a linear relation:

$$Q_{pump,t} = B_{pump,t} (h_{i,t} - h_{i+1,t}) + A_{pump,t} \quad (48)$$

with:

$Q_{pump,t}$	pump discharge	[$m^3 \cdot s^{-1}$]
$B_{pump,t}$	slope of pump function	[$m^3 \cdot s^{-1}$]
$A_{pump,t}$	pump constant	[$m^3 \cdot s^{-1}$]

$A_{pump,t}$ and $B_{pump,t}$ must be defined by the user. If $B_{pump,t}$ is set to zero, the equation further simplifies to a constant given discharge equal to $A_{pump,t}$.

Pump control
Three options for pump control can be applied:

- Fixed discharge per period:
  For a certain period A_{pump} is defined by the user. B_{pump} is set to 0.

- Upstream start and stop level per period:

If $h_{i,t} > h_{start,upstream(i-1)}$ pumping is started using A_{pump} and B_{pump} until $h_{i,t} < h_{stop,upstream(i-1)}$

- Downstream start and stop level per period:
  If $h_{i+1,t} > h_{start,downstream(i+1)}$ pumping is started using A_{pump} and B_{pump} until $h_{i+1,t} < h_{stop,downstream(i+1)}$

Moreover, the pump discharge is linearly reduced when the upstream water depth drops below 0.5 m. Below a depth of 0.25 m pumping is stopped completely.

3.4 Boundary conditions

Several boundary conditions can be imposed on the nodes, being the basic computational units in SWQN. At present six different boundary conditions are included that can act, in principle, simultaneously on a node. The boundary conditions can be defined in two groups, imposed heads and fluxes.

Head

1. Fixed water level calculated with:

$$h_{node,t} = constant_t \qquad \text{in [m]} \qquad (49)$$

Fluxes

2. A sink/source can be calculated with the method:

$$Q_{node,t} = constant_t \qquad \text{in [m}^3\text{ s}^{-1}\text{]} \qquad (50)$$

An example of a source is the discharge of effluent by a factory. A sink could be a withdrawal from a drinking water plant (if not modeled as a pump).

3. Infiltration or drainage (in exchange with the subsoil) per m^2 of wetted profile can be calculated with the method:

$$q_{infiltration/drainage} = \frac{\left(h_{phreaticgroundwater} - h_{node,t}\right)}{c_{drain}} + constant \quad \text{in [m s}^{-1}\text{]} \qquad (58)$$

where c_{drain} stands for the drainage resistance [s] while the constant usually is set to zero. The function can be made constant by letting c_{drain} approach infinity and giving the constant a value per time period. Multiplication with the wetted profile gives the total in- or outgoing flux.

4. Leakage or seepage (interaction with the groundwater) per m^2 of wetted profile is calculated with a different method in which the groundwater head is

not explicitly expressed. Instead a linear function is defined based on the surface water level in the node itself according to:

$$q_{leekage/\,seepage} = C_1 h_{node,t} + C_2 \quad \text{in [m s}^{-1}\text{]} \qquad (51)$$

Multiplication with the wetted profile gives again the total in- or outgoing flux.

5. A fixed Q-h relation is calculated as:

$$Q_{Q-h,t} = C_1 h_{node,t} + C_2 \qquad \text{in [m}^3\text{ s}^{-1}\text{]} \qquad (52)$$

Examples are for instance an external pump.

6. Precipitation and evaporation from open water can be important components in the water balance. They are usually expressed in mm, but are here given in m per unit time. By multiplying the terms with the surface area and time step the model calculates the net precipitation volume per time step:

$$P_{node,t} = precipitation = constant \text{ in [m] per time interval} \qquad (61)$$

$$E_{openwater,t} = open\ water\ evaporation = constant \text{ in [m] per time interval} \qquad (71)$$

For the surface area the area at MAXLEVEL is taken (

Figure 6). Hence, rainfall and evaporation from the (variable) freeboard are included in the nodal water balance.

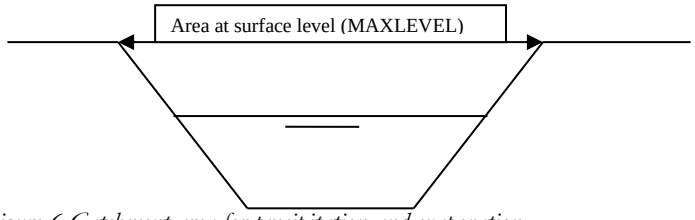

Figure 6 Catchment area for precipitation and evaporation

The precipitation and evaporation are specified per meteorological region. The region has to be specified per node.

For all flux boundary conditions cut-off values are included when water levels approaches the bottom of the water course or the land surface level.

4 Solution scheme

4.1 Mathematical solution for the flow equations

The equation for mass conservation reads on nodal basis as:

$$\frac{dV_i}{dt} = \sum_{j=1,\, j\neq i}^{n_i} Q_{i,j} + \sum_{k=1}^{nb_k} Qb_{i,k} \tag{53}$$

where:

V_i	Water volume in node i	m^3
$Q_{i,j}$	Incoming waterflow for node i from node j	$m^3\ s^{-1}$
$Qb_{i,k}$	Incoming waterflow for node i from boundary k	$m^3\ s^{-1}$
n_i	Number of adjacent nodes to node i	-
nb_k	Number of boundary flows to node i	-

The water volume in node i is a function of time. The linearized relation can be written as:

$$V_i(t) = A_i(h_{i,0})\, h_i(t) \tag{54}$$

where $h_{i,0}$ is the water level at the start of the time step. The water flow between node i and its neighbor node j follows from:

$$Q_{i,j} = \alpha_{i,j}(h_{i,0}, h_{j,0})\left(h_j - h_i\right) \tag{55}$$

The conductance coefficient $\alpha_{i,j}(h_{i,0},h_{j,0})$ in $m^2\ s^{-1}$ is calculated from the linearized Chézy equation (Eq. 23). Its value is based on the initial water level for the current time step. The boundary flows for node i can be written as:

$$Qb_{i,k} = \beta_{i,k}(h_{i,0})(p_{i,k} - h_i) + \Phi_{i,k} \tag{56}$$

where

$\beta_{i,k}(h_{i,0})$	Linearized conductance coefficient for a water level dependent boundary flow	$m^2\ s^{-1}$
$p_{i,k}$	Water level at the boundary k for node i	m
$\Phi_{i,k}$	Boundary flow independent from the water level at node i	$m^3\ s^{-1}$

Substitution of equations (63), (64) and (65) into (62) yields:

$$A_i(h_{i,0})\frac{dh_i}{dt} = \sum_{j=1,\, j\neq i}^{n_i} \alpha_{i,j}(h_{i,0}, h_{j,0})\left(h_j - h_i\right) + \sum_{k=1}^{nb_k}\left(\beta_{i,k}(h_{i,0})(p_{i,k} - h_i) + \Phi_{i,k}\right) \tag{57}$$

Rewriting gives:

$$A_i(h_{i,0})\frac{dh_i}{dt}+\left(\sum_{j=1,j\neq i}^{n_i}\alpha_{i,j}(h_{i,0},h_{j,0})+\sum_{k=1}^{nb_k}\beta_{i,k}(h_{i,0})\right)h_i=$$
$$\sum_{j=1,j\neq i}^{n_i}\alpha_{i,j}(h_{i,0},h_{j,0})\,h_j+\sum_{k=1}^{nb_k}\left(\beta_{i,k}(h_{i,0})p_{i,k}+\Phi_{i,k}\right) \tag{58}$$

With time averaged values $\bar{h}_j$ for the water levels of the adjacent nodes and some rewriting again Eq. 67 morphs into:

$$\frac{dh_i}{dt}+\frac{\left(\sum_{j=1,j\neq i}^{n_i}\alpha_{i,j}(h_{i,0},h_{j,0})+\sum_{k=1}^{nb_k}\beta_{i,k}(h_{i,0})\right)}{A_i(h_{i,0})}h_i=$$
$$\frac{\sum_{j=1,j\neq i}^{n_i}\alpha_{i,j}(h_{i,0},h_{j,0})\,\bar{h}_j}{A_i(h_{i,0})}+\frac{\sum_{k=1}^{nb_k}\left(\beta_{i,k}(h_{i,0})p_{i,k}+\Phi_{i,k}\right)}{A_i(h_{i,0})} \tag{59}$$

The solution of this first order differential equation reads:

$$h_i(t)=h_{i,0}e^{-\lambda_i t}+\frac{\sum_{j=1,j\neq i}^{n_i}\alpha_{i,j}(h_{i,0},h_{j,0})\quad\bar{h}_j}{\sum_{j=1,j\neq i}^{n_i}\alpha_{i,j}(h_{i,0},h_{j,0})+\sum_{k=1}^{nb_k}\beta_{i,k}(h_{i,0})}\left(1-e^{-\lambda_i t}\right)+$$
$$\frac{\sum_{k=1}^{nb_k}\left(\beta_{i,k}(h_{i,0})p_{i,k}+\Phi_{i,k}\right)}{\sum_{j=1,j\neq i}^{n_i}\alpha_{i,j}(h_{i,0},h_{j,0})+\sum_{k=1}^{nb_k}\beta_{i,k}(h_{i,0})}\left(1-e^{-\lambda_i t}\right) \tag{60}$$

with λ equal to:

$$\lambda_i=\frac{\left(\sum_{j=1,j\neq i}^{n_i}\alpha_{i,j}(h_{i,0},h_{j,0})+\sum_{k=1}^{nb_k}\beta_{i,k}(h_{i,0})\right)}{A_i(h_{i,0})}$$

A time averaged value for the water level at node *i* is then found by integration and division by the length of the time step T:

$$\bar{h}_i = h_{i,0}\left(\frac{1-e^{-\lambda_i T}}{\lambda_i T}\right) + \frac{\sum_{j=1,\, j\neq i}^{n_i} \alpha_{i,j}(h_{i,0}, h_{j,0})\,\bar{h}_j}{\sum_{j=1,\, j\neq i}^{n_i} \alpha_{i,j}(h_{i,0}, h_{j,0}) + \sum_{k=1}^{nb_k} \beta_{i,k}(h_{i,0})}\left(1-\frac{1-e^{-\lambda_i T}}{\lambda_i T}\right) + \frac{\sum_{k=1}^{nb_k}\left(\beta_{i,k}(h_{i,0})\,p_{i,k} + \Phi_{i,k}\right)}{\sum_{j=1,\, j\neq i}^{n_i} \alpha_{i,j}(h_{i,0}, h_{j,0}) + \sum_{k=1}^{nb_k} \beta_{i,k}(h_{i,0})}\left(1-\frac{1-e^{-\lambda_i T}}{\lambda_i T}\right) \tag{61}$$

For all nodes within a network these interdependencies of water levels can be expressed as a set of linear equations:

$$\begin{pmatrix} a_{1,1} & a_{1,2} & \cdots & a_{1,i} & \cdots & a_{1,n-1} & a_{1,n} \\ a_{2,1} & a_{2,2} & & & & a_{2,n-1} & a_{2,n} \\ \vdots & & \ddots & & \iddots & & \vdots \\ a_{i,1} & a_{i,2} & & a_{i,i} & & & \\ \vdots & & \iddots & & \ddots & & \vdots \\ a_{n-1,1} & a_{n-1,2} & & & & a_{n-1,n-1} & a_{n-1,n} \\ a_{n,1} & a_{n,2} & \cdots & a_{n,i} & \cdots & a_{n,n-1} & a_{n,n} \end{pmatrix} \begin{pmatrix} \bar{h}_1 \\ \bar{h}_2 \\ \vdots \\ \bar{h}_i \\ \vdots \\ \bar{h}_{n-1} \\ \bar{h}_n \end{pmatrix} = \begin{pmatrix} b_1 \\ b_2 \\ \\ b_i \\ \\ b_{n-1} \\ b_n \end{pmatrix}$$

(62)

where the coefficients of the matrix are given by:

$$a_{i,i} = 1; \qquad for \quad i \neq j: \quad a_{i,j} = \frac{\alpha_{i,j}(h_{i,0}, h_{j,0})\left(1-\frac{1-e^{-\lambda_i T}}{\lambda_i T}\right)}{\sum_{j=1,\, j\neq i}^{n_i} \alpha_{i,j}(h_{i,0}, h_{j,0}) + \sum_{k=1}^{nb_k} \beta_{i,k}(h_{i,0})}$$

and the coefficients of the right hand side vector by:

$$b_i = h_{i,0}\left(\frac{1-e^{-\lambda_i T}}{\lambda_i T}\right) + \frac{\sum_{k=1}^{nb_k}\left(\beta_{i,k}(h_{i,0})\,p_{i,k} + \Phi_{i,k}\right)}{\sum_{j=1,\, j\neq i}^{n_i} \alpha_{i,j}(h_{i,0}, h_{j,0}) + \sum_{k=1}^{nb_k} \beta_{i,k}(h_{i,0})}\left(1-\frac{1-e^{-\lambda_i T}}{\lambda_i T}\right)$$

In a very simplified way Eq. 81 can also be written as:

$$[A]\left[\vec{h}\right]=[B] \tag{63}$$

The matrix [A] has a sparse shape with unity on the main diagonal and as many non-zero coefficients on row *i* as node *i* has connections to neighboring nodes. Optimum use of these properties is made when such a scheme is solved with an appropriate solver based on Gauss elimination or other methods.

For each time step T Equation 71 (or 72) is solved for all nodes and the time averaged water levels are substituted in Equation 69 to obtain the water levels at the end of the time step. Due attention, however, should be given to the fact that water surface A_i is based on the initial water level at the beginning of the time step (Eq. 67). For cross sections where this area depends on the water level itself (e.g. trapezoids), changes in these levels will cause errors in the nodal water balance when not corrected. To circumvent such errors, an iteration procedure is applied that uses an averaged water level. This scheme converges rapidly towards minimal water balance deviations, generally within three iteration steps.

4.2 Notes on the solution scheme

The solution for Equations 71-72 is robust but causes problems when the matrix [A] becomes singular. Such a situation will occur when two nodes are linked by two parallel connectors with the same hydraulic properties. Solutions can be applied in the software or the input data by, for instance, slightly modifying the properties of one of the convectors or removing one or more of them all together.

In surface water systems water courses dry up frequently. When the water level approaches the bottom of the water course flow will stop. Under such conditions the numerical schemes could result in new computed water levels below the nodal bottom. This results then in a negative storage in the node together with an over-estimated flow to neighboring nodes.

Several correctional procedures can be applied, each with its own advantages and disadvantages. A simple workaround is to a priori reduce the length of the time when the water level approaches a preset critical level. As this measure will affect the whole computational scheme model performance will degrade.

Another, posterior, measure is to correct flows from node *i* after dry fall has occurred. This would affect performance less, but requires a re-calculation of the complete scheme to refill the dried up nodes.

A third widely used procedure, which has not yet been made operational in SWQN, is to modify the cross profile into a conical shape after a threshold water depth has been reached. Such a shape will sharply reduce flows and therefore also limit negative storage.

5. Model verification

5.1 Introduction

To gain insight in the accuracy and stability of the solution yielded by the SWQN model in comparison to other, more sophisticated models, we followed the approach presented in the article by Contractor and Schuurman (1993). The first test in this article checks the models ability to conserve mass. The second test concerns the so-called 'ramp-discharge' test. Both tests are applied to five different models based on the full Saint-Venant equations. All models use an implicit solution scheme and are, therefore, unconditionally stable. It is also shown in the article that the accuracy depends on the Courant number, in which time-step size, distance-step size, wave celerity and flow velocity are represented. Courant numbers approaching unity yield the most accurate solutions for models with implicit solution schemes. In practice, the time-step size is used to control the desired accuracy.

5.2 Setup

Mass-conservation test
The mass-conservation test shows the ability of a model to conserve mass. A sinusoidal boundary condition is applied for one period onto a horizontal trapezoidal channel with a dead-end. This results in a net inflow of zero. The calculation is then continued with no inflow, and after the wave activity has ceased, the final water depth is compared with the initial depth. Ideally the error should be zero. The details of the mass-conservation test are as follows:

- Canal Geometry: horizontal, prismatic canal 10 km in length, trapezoidal cross section, base width = 10 m, side slopes of 2 horizontal to 1 vertical. Manning coefficient = 0.04;
- Numerical Discretization: 11 computational points, spaced at equal intervals of 1 km. Constant time step of 6 minutes;
- Initial Condition: zero flow, constant water depth of 7 m above canal invert;
- Boundary Conditions: no downstream discharge (i.e. dead-end canal); upstream we have $Q = 200 \sin(2\pi t/21600)$ m^3/s where t is in seconds, for a period between $0 \leq t \leq 6$ hours; $Q = 0$ m^3/s for $t > 6$ h. A positive Q means that flow is pumped into the canal and a negative Q means that water is pumped out of the canal.

Ramp-discharge test
The ramp-discharge test shows how various models react to a fivefold flow increase within a 10 minutes period in a prismatic mildly sloping canal. Output at various time-step sizes is studied. The article by Contractor and Schuurman (1993) also included the DUFLOW model. Since its results appeared rather bad it was decided to include the latest version in the simulations.

The details of the test with ramp discharge as inflow are as follows:

- Canal Geometry: trapezoidal section; base width = 9.144 m (30 ft); side slopes of two horizontal to one vertical; length = 3219 m (2 mi); longitudinal slope = 1 in 2000; Manning coefficient = 0.02;
- Numerical Discretization: 21 computational point, spaced at equal intervals of 160.9 m (0.1 mi); time step Δt = 10, 5, 2 and 1 min; weighting factor θ = 0.60;
- Initial Condition: Q = 28.32 m^3/s (1000 cfs); normal depth of 1.707 m (5.6 ft) along the canal;
- Boundary Condition: upstream flow increases linearly from 28.32 m^3/s (1000 cfs) to 141.6 m^3/s (5000 cfs); downstream Manning equation satisfied.

The downstream boundary (condition satisfying the Manning equation) is not directly available as an option in both SURFACEWATER and DUFLOW. Therefore we fulfilled this condition by extending the canal tenfold with at the downstream end a constant level boundary. Is has been proven that this set-up does not affect the flow at the 21st node, hence satisfying the Manning boundary condition.

5.3 Results

Mass-conservation test

Because SURFACEWATER is based on mass-conservation, the model shows no mass-balance errors. This result was only achieved by two other models: DUFLOW and MODIS (Table 2).

Table 2: Results of Mass Conservation Test (after Contractor and Schuurman (1993); extended)

Name of model	Error (%)	Remarks
CANAL	0.004	
CARIMA	0.91	θ = 1.0; no iterations
	0.023	θ = 0.55; <3 iterations
USM	0.05	
SNUSM	0.07	Amplitude of Q = 20 m^3/s
DUFLOW (old version)	0.90	θ = 1.0; no iterations
	0.0	θ = 0.55; <3 iterations
MODIS	0.0	For 2 iterations/time step
	0.57	For one iteration
SURFACEWATER	0.0	

Ramp-discharge test

To enable a direct comparison we scanned the graphs from the original article and superimposed our new results onto them (Figure 7 to 12). Due to its solution scheme based on the method of characteristics, USM is considered as the most accurate model and is hence used as a reference. For the largest time-step of 10 minutes two

models show oscillations (old DUFLOW and MODIS). The models CANAL and CARIMA show minor numerical dispersion, while DUFLOW 3.6 and SURFACEWATER demonstrate somewhat more numerical dispersion. A further decrease in time-step size till 2 minutes and finally 1 minute gives acceptable results for all models with the exception of the old DUFLOW (still major numerical dispersion) and to a minor extent DUFLOW 3.6 which shows some slight dispersion.

Other tests with SURFACEWATER have demonstrated that even for time-step sizes of 30 minutes and beyond, the numerical solution scheme produces stable, i.e. non-oscillating, results (see Figure 11). However, large numerical dispersion under such conditions should be accepted.

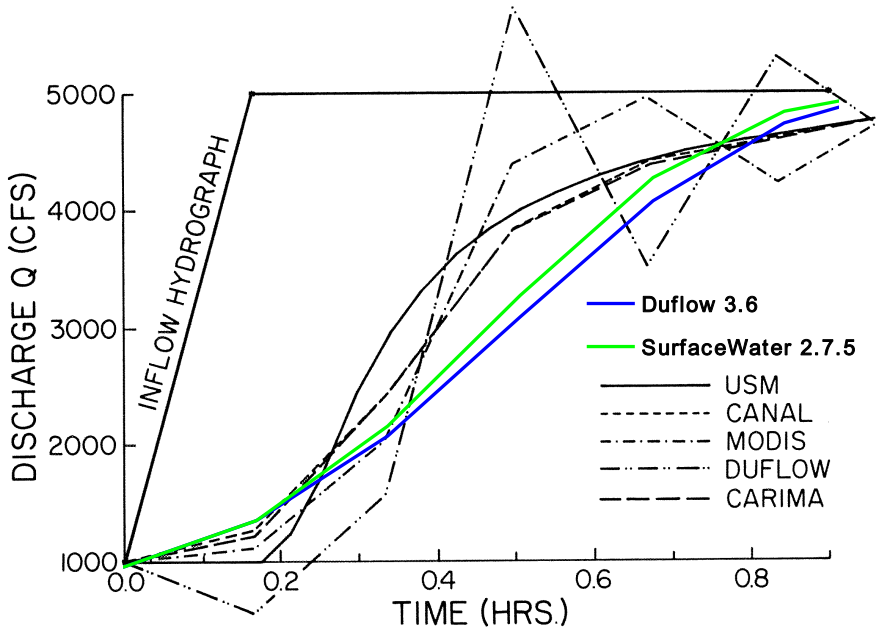

Figure 7 Comparison of model outputs: Time Step = 10 min; Courant Number = 18.4

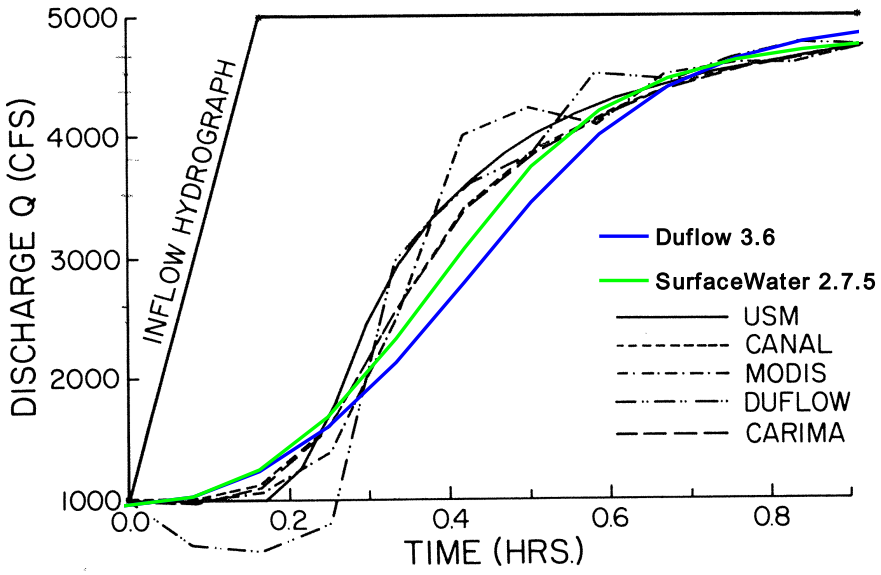

Figure 8 Comparison of model outputs: Time Step = 5 min; Courant Number = 9.22

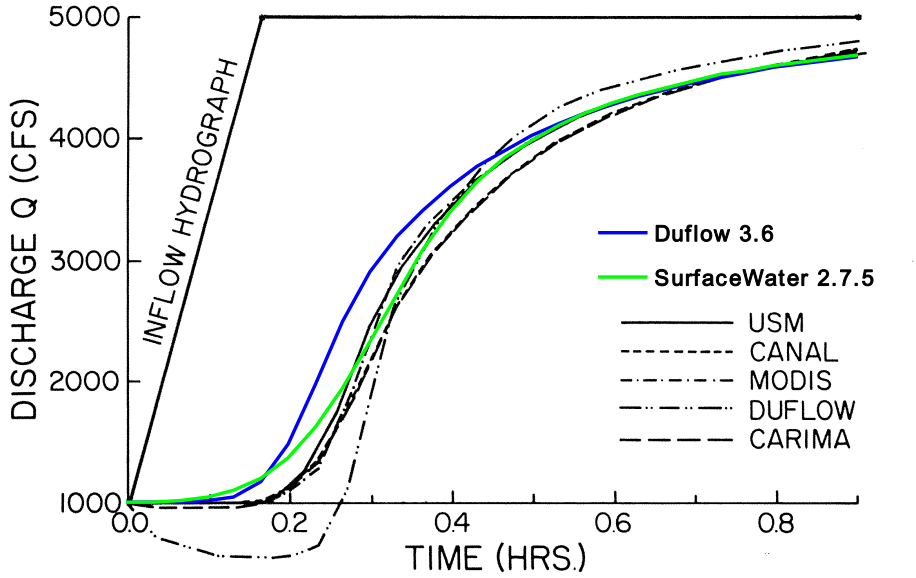

Figure 9 Comparison of model outputs: Time Step = 2 min; Courant Number = 3.69

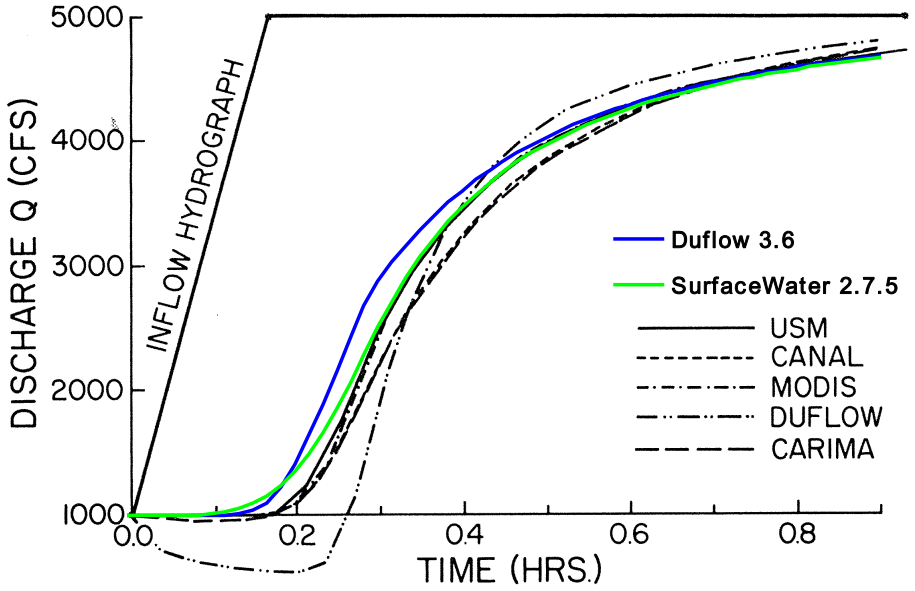

Figure 10 Comparison of model outputs: Time Step = 1 min; Courant Number = 1.84

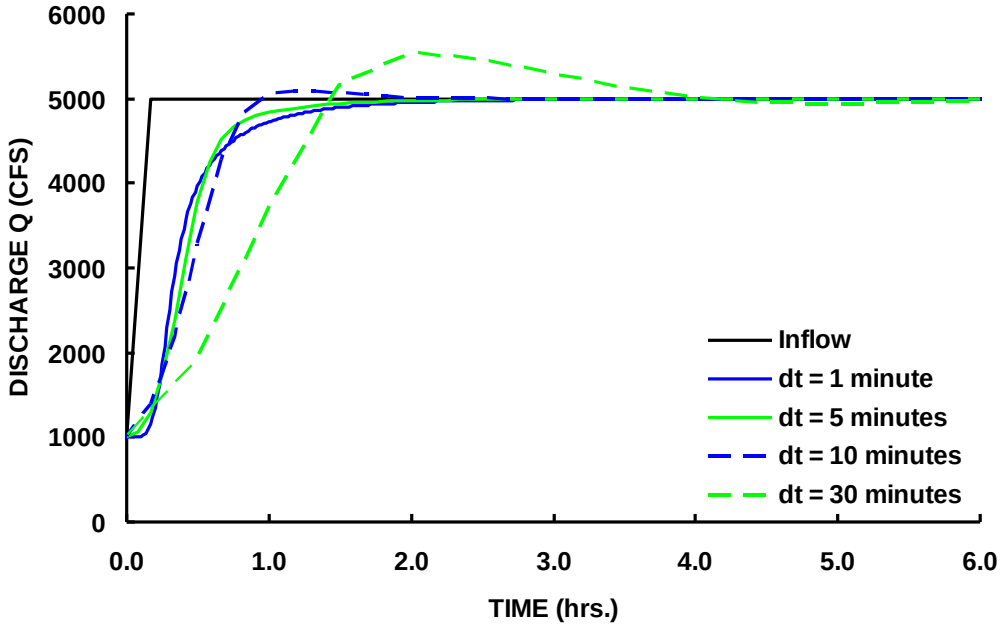

Figure 11 Comparison of SURFACEWATER results at various time steps

5.4 Domain assessment for application

Clearly, SURFACEWATER can produce a similar accuracy as the best models based on the full Saint-Venant equations for time-step sizes in the order of one to several minutes for simple non-steady state non-uniform flows in prismatic channels. Its robustness has been demonstrated by using very large time steps which still result in smooth solutions without oscillations or, in extreme cases, model crashes. However, use of larger time-steps does lead to significant numerical dispersion, which may not always be acceptable. On the other hand, elongated time steps together with the linearized solution scheme warrants fast computations for extended networks.

SURFACEWATER cannot solve supercritical flow and associated hydraulic jumps and bore waves, although it can handle the advance on a dry bed, channel de-watering, reverse flows, negative flows at structures, and rapid flow changes.

So far, its use remained restricted to the simulation of large irrigation schemes and (scenario type) regional studies within the Netherlands and Europe with a focus on discharges based on daily or 10-daily averaged inputs, such as drainage and abstractions (Smit and Abdel Gawad, 1993; Schoumans *et al.*, 2005). This application scale implies that effects from local hydraulic phenomena or numerical dispersion would hardly play a role. In addition, water management in irrigated agriculture and in the Netherlands require due attention for water level or discharge control at the dense network of structures. These have been fully incorporated in SWQN.

Considering these aspects, the major field of application for the SWQN model lies in regional studies. However, also more detailed studies on smaller time- and spatial scales appear feasible, where significant improvements over other models in execution time could be obtained. This would allow for instance assessments of lag-time distributions of water quality parameters after loading the water system with point loads, insofar no complicated hydraulic phenomena are encountered.

Literature

Abdel Gawad, S.T., M.A. Abdel Khalek, D. Boels, D.E. El Quosy, C.W.J. Roest, P.E. Rijtema, M.F.R. Smit, 1991. Analysis of Water Management in the Eastern Nile Delta. Reuse of Drainage Water Project Report 30. Drainage Research Institute, Qanater, Cairo, Egypt and The Winand Staring Centre, Wageningen, The Netherlands.

Bos, M.G., 1978. Discharge measurement structures. International Institute for Land Reclamation and Improvement (ILRI), Wageningen.

CTV, Werkgroep herziening cultuurtechnisch vademecum, 1988. Cultuur Technisch Vademecum. Cultuurtechnische Vereniging, Utrecht, The Netherlands.
In English: Working group review handbook agricultural engineering, 1988.

Contractor, D. N., and W. Schuurmans (1993). Informed use and potential pitfalls of canal models. Journal of irrigation and drainage engineering 119(4), 663-672.

Dik, P.E., M.H.J.L. Jeuken, L.P.A. van Gerven, 2009. SWQN, Manual version 3.0. Alterra Report 1226.3, Wageningen.

Dik, P.E., J.G. Kroes, A.A.M.F.R. Smit, A.A. Veldhuizen, 2005. Onderbouwing wateropgave Haarlemmermeerpolder; modelbouw, kalibratie en scenarioanalyse. Alterra Rapport 1183. Alterra, Wageningen.
In English: Proofing the water management plan for the Haarlemmermeer polder: model building, calibration, and scenario analyses.

Dik, P.E., J.G. Kroes, A.A.M.F.R Smit, 2004. Water- en zoutbeheer Polder de Noordplas: schematisatie, parameterisatie en verkennende scenarioanalyse. Alterra rapport 986. Alterra, Wageningen.
In English: Water and salt management in the polder Noordplas: schematization, parametrization, and scenario analysis.

Gelok, A.J., 1969. Opstuwing duikers. Cultuurtechnisch Tijdschrift 9(3), 132-140.
In English: Backwater at divers. Journal for Agricultural Engineering 9(3), 132-140.

Groenendijk, P., M. van Elswijk, J. Huygen, J.G. Kroes, A.J. Otjens, A.A.M.F.R. Smit, A.A. Veldhuizen, and J.G. Wesseling, 1999. MultiSwap als applicatie van het Framework Integraal Waterbeheer. Techn. Doc. 60, The Winand Staring Centre, Wageningen.
In English: MultiSwap as application of the Framework Integrated Water management.

Henderson, F.M., 1966. Open channel flow. The MacMillan Company, New York.

Kroes, J.G., P.E. Dik, H. Van Hardeveld, and R. Smit, 2004. Balancing water and salt flow in a Dutch polder using an integrated modelling system. In: Symposium "Unsaturated zone modeling: progress, challenges and applications"; poster abstracts. – Wageningen: Frontis, Farewell symposium in honour of the retirement of Prof. Reinder Feddes, 2004-10-03/ 2004-10-05.

Rijtema P.E., M.F.R. Smit, D. Boels, S.T. Abdel Gawad, and D.E. El Quosy, 1991. Formulation of the Water Distribution Model WATDIS. Reuse of Drainage Water Project Report 23. Drainage Research Institute, Cairo, Egypt and The Winand Staring Centre, Wageningen, The Netherlands.

Schoumans O.F., C. Siderius, and P. Groenendijk, 2009. NL-CAT application to six European catchments. Alterra report 1205, Alterra, Wageningen.

Smit, M.F.R. and S.T. Abdel Gawad, 1992. Irrigation water distribution in the Nile Delta: A model approach. In: Proceedings of a workshop on water management in irrigated agriculture, Abdel Gawad S.T. and M.F.R. Smit (Eds.), 91-107, Cairo, Egypt.

Torfs, 2000. Stroming in open waterlopen. Collegedictaat, Wageningen University and Research Center, Wageningen.
In English: Flow in open channels. Lecture notes Wageningen University.

Ven Te Chow, 1959. Open-Channel Hydraulics. Mcgraw-Hill, New York.

Visser, T.N.M., W. Wolters, M.F.R. Smit, and M.A. Abdel Khalek, 1993. Simulated irrigation efficiencies in the Eastern Nile Delta. In: Transactions - Fifteenth congress on irrigation and drainage, The Hague, on the theme 'Water management in the next century', ICID, Vol.1-D, 1485-1500.

Weinmann, P. E., and E. M. Laurenson, Approximate flood routing methods: A review, *J. Hydraulic Div.*, ASCE, 105 (HY13), Proc., Paper 15057, 1979.

Appendix 1 Parameters

$A_{j,t}$	wetted cross profile of the segment [m^2]
$A_{i,i}$	water surface area of node i [m^2]
$A_{undershot,t}$	gate opening [m^2]
$A_{pump,t}$	pump constant [$m^3 \cdot s^{-1}$]
A	NxN matrix [-]
a	number of parallel culverts[-]
a	wetted cross profile of the culvert divided by the wetted cross profile of the downstream water course[-]
$a_{i+1,t}$	iterative factor for node i ($0 \leq \alpha_{i+1,t} \leq 1$) [-]
$B_{pump,t}$	slope of pump function [$m^3 \cdot s^{-1}$]
b_j	Width at the bottom of section j [m]
C_d	discharge efficiency coefficient [-] ~ 1.0 to 1.25 for short crested weir ~ 0.848 for broad crested weir (Bos, 1978)
C_v	velocity correction coefficient[-] ~ 1.0 to 1.1 for short and broad crested weirs (Bos, 1978)
C_d	discharge efficiency coefficient estimated at 0.85 [-]
C_v	velocity correction coefficient estimated at 1.035[-]
$C_{Chézy,j}$	de Chézy coefficient [$m^{1/2}\ s^{-1}$]
g	Acceleration due to gravity [ms^{-2}]
$\Delta H_{i,i+1,t}$	difference in energy head between nodes i and i+1 [m^+ref]
h	Water level [m]
$h_{i,t,corrected}$	corrected water level in node i [m^+ref]
$h_{i,t}$	upstream water level [m]
$h_{crest,t}$	crest level [m]
$h_{centre,t}$	level of the centre of the gate opening at the upstream side [m]
$\Delta h_{j,t}$	Difference in water level over segment j [m]
h	vector with the solution for the water levels $h_{i,t}$ at time $t=t+\Delta t$ [m]
$h_{i+1,t,av}$	average approximated water depth in section j+1 [m]
$h_{i+1,t+\Delta t}$	water depth in section k+1 at time $t = t + \Delta t$ [m]
k_m	Manning coefficient [$m^{1/3}\ s^{-1}$], same as $1/n_{manning}$
L	length of culvert [m]
ΔL_j	distance between nodes i and i+1 [m]
L_j	Length of section j [m]
$Q_{i-1,i,t}$	flow from node i-1 to node i [$m^3 \cdot s^{-1}$]
$Q_{i,i+1,t}$	flow from node i to node i+1 [$m^3 \cdot s^{-1}$]
$\Sigma Q_{i,t}$	sum of sink and/or source terms for node i [$m^3 \cdot s^{-1}$]
$Q_{j,t}$	flow in segment j at time t [$m^3\ s^{-1}$]
$Q_{undershot,t}$	discharge of free flow undershot gate at time t [$m^3 \cdot s^{-1}$]
$Q_{weir,t}$	weir discharge at time t
$Q_{pump,t}$	pump discharge [$m^3 \cdot s^{-1}$]
$Q_{j,t}$	flow in segment j at time t [$m^3\ s^{-1}$]
R	Hydraulic radius [m]
RHS	vector with the Right Hand Side of the equations [m]
$S_{j,begin}$	Slope at the begin of section j [-]
s_j	slope in bottom level [-]
$S_{j-1,end}$	Slope at the end of section j-1 [-]
S_o	Bed slope [-]

$s^1_{e,j,t}$	slope in energy head for segment j at time t [-]
Δt	time step [s]
v	Velocity [ms^{-1}]
$V_{i,t}$	water volume in node i at time t [m^3]
W_{crest}	crest width [m]
z	height to reference level (m)
k	shape coefficient for the outlet [-] - k=1 if all kinetic energy is dissipated - k=0 if no energy losses occur
μ	combined resistance coefficient [-]
ξ_e	entry resistance [-] ~ 0.6 for round shaped culverts (CTV, 1988) ~ 0.5 for square shaped culvert
ξ_f	friction coefficient [-]
ξ_o	coefficient for outlet losses [-]

Appendix 2 Flow in open conduits - St. Venant equations

The unsteady flow in open waters was first described by St. Venant in 1848. His well-known St. Venant equations consist of two parts: i) the conservation of mass and ii) the energy or momentum balance in one dimension for a water body of infinitesimal length.

The continuity equation

In Figure 1 a schematization of a short length (dx) of a prismatic surface water channel is shown.

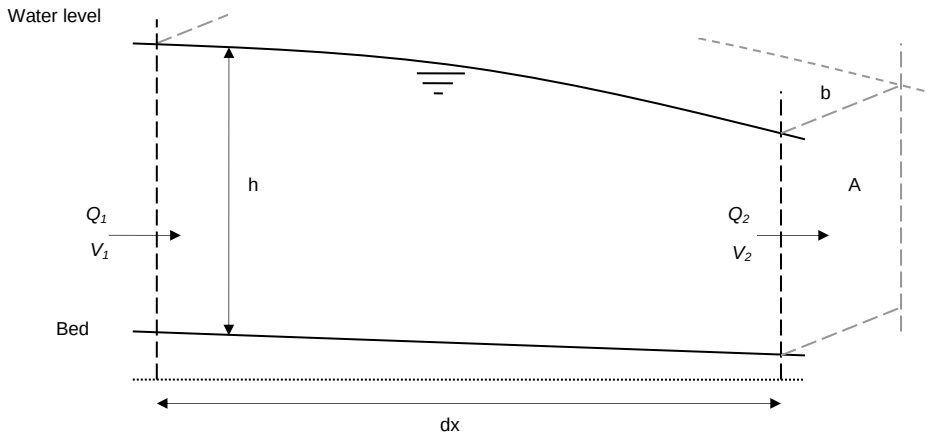

Figure 12 Flow through a part (dx) of the surface schematization

The continuity equation, describing the conservation of mass, can easily be derived for this section. In unsteady flow in open water the discharge changes with distance:

$$Q_2 - Q_1 = \frac{\partial Q}{\partial x} dx \qquad (1)$$

where:

Q_1	discharge through section 1	[$m^3 s^{-1}$]
Q_2	discharge through section 2	[$m^3 s^{-1}$]

which can also be described as:

$$\frac{\partial Q}{\partial x} dx = \frac{\partial (Av)}{\partial x} dx = v \frac{\partial A}{\partial x} dx + A \frac{\partial v}{\partial x} dx \qquad (2)$$

where:

A	cross sectional area	[m^2]
v	mean velocity at the section	[m^2 s^{-1}]

At the same time the volume of water between sections 1 and 2 changes with time at a rate:

$$\frac{\partial A}{\partial t} dx = b \frac{\partial h}{\partial t} dx \qquad (3)$$

where:

b	width of the section	[m]
h	water level	[m]
t	time	[s]

The continuity equation, when assuming no lateral inflow of water, then becomes:

$$v \frac{\partial A}{\partial x} + A \frac{\partial v}{\partial x} + b \frac{\partial h}{\partial t} = 0 \qquad (4)$$

The dynamic equation

Next to the mass of conservation rule Newton's second law can be applied:

Force = mass × acceleration

Due to the change in velocity over time there will be work done by an acceleration force over a distance *dx*:

$$W_a = F_a dx = \frac{w}{g} \frac{\partial v}{\partial t} dx \qquad (5)$$

where:

W_a	work done by acceleration force	[Nm]
F_a	acceleration force	[kg m s^{-2}]
w	weight	[kg m s^{-2}]
g	acceleration due to gravity	[m s^{-2}]
v	velocity	[m s^{-1}]

Dividing by mass (*w*) gives the head loss (*h*) (**Error! Reference source not found.**). Similar to steady flow there will also be a frictional resistance of channel walls and bed. The total loss in head will thus consist of two parts:

the loss due to acceleration:

$$h_a = \frac{1}{g} \frac{\partial v}{\partial t} dx \qquad (6)$$

and the loss due to friction:

$$h_f = S_f\,dx \tag{7}$$

where S_f is the friction slope (-). A change in head can be described by these two terms as is shown in **Error! Reference source not found.** and equation 8.

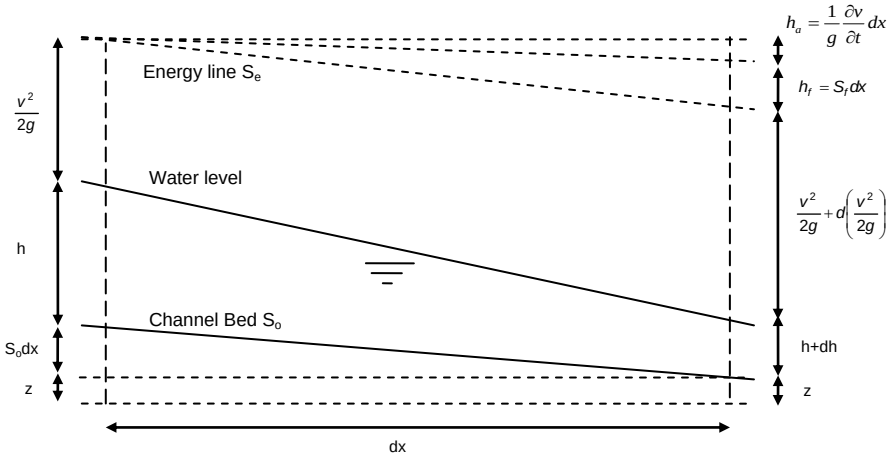

Figure 13 Simplified representation of energy in unsteady flow

By the energy principle it follows:

$$z + S_o\,dx + h + \frac{v^2}{2g} = z + h + dh + \frac{v^2}{2g} + d\left(\frac{v^2}{2g}\right) + \frac{1}{g}\frac{\partial v}{\partial t}dx + S_f\,dx \tag{8}$$

where:

z	height above reference level	[m]
S_o	bed slope	[-]
v	velocity	[m s^{-1}]
h	water level	[m]
g	acceleration due to gravity	[m s^{-2}]

Simplifying gives:

$$d\left(h + \frac{v^2}{2g}\right) - S_o\,dx = -\frac{1}{g}\frac{\partial v}{\partial t}dx - S_f\,dx \tag{9}$$

The left side represents the change in total head. The two terms on the right are the head losses due to acceleration and friction. Dividing by *dx,* multiplying by *g* and rearranging gives the dynamic (or momentum) equation, which constitutes the second part of the St. Venant equations:

$$g\frac{\partial h}{\partial x} + v\frac{\partial v}{\partial x} + \frac{\partial v}{\partial t} = g(S_o - S_f) \qquad (10)$$

Equations 4 and 10 together form the St. Venant equations describing unsteady flow in open waters. These dynamic wave equations are considered to be the most accurate and comprehensive solution to 1-D unsteady flow problems in open channels. Nonetheless, these equations are based on specific assumptions, and therefore have limitations. The assumptions used in deriving the dynamic wave equations are as follows:

- Velocity is constant and the water surface is horizontal *across* any channel section perpendicular to the longitudinal axis;
- All flows are gradually varied with hydrostatic pressure prevailing at all points along the longitudinal axis, such that vertical accelerations can be neglected;
- Channel boundaries are treated as fixed; therefore, no erosion or deposition occurs;
- The slope of the channel bottom is small;
- Water is of uniform density, and resistance to flow can be described by empirical formulas, such as the Manning or the Chézy equations;
- The flow is incompressible and homogeneous in density.